A first-order qP-wave propagator in 2D vertical transversely isotropic (VTI) media

He. Liu, Kristopher. Innanen

ABSTRACT

In a vertical transversely isotropic (VTI) medium, quasi-P (qP) and quasi-SV (qSV) waves are intrinsically coupled as described in elastic wave equations. Therefore, when we perform elastic reverse time migration and imaging processes to qP-waves, qSV-wave energy will introduce crosstalk noise to the imaging results. Many authors have proposed to separate qP-waves from elastic waves for better imaging results. As an alternative way, some authors have proposed to directly simulate qP-waves with modified elastic wave equations. In this study, we develop a first-order wave propagator of pseudo-pure-qP-wave in 2D heterogeneous VTI media using staggered-grid scheme. We have performed this algorithm to simulate P-waves propagating in an isotropic medium, VTI media with weak/strong anisotropy and a two-layer VTI model, the synthetic results validate the feasibility of this algorithm. Also, we adopt the first-order Hybrid-PML in the simulation, which helps the simulation efficiency due to its better performance for anisotropic media.

INTRODUCTION

Elastic reverse time migration (ERTM) can provide more accurate underground geological structures than the acoustic RTM (Chang and McMechan, 1987). However, in VTI media, P- and S-waves are coupled, which introduces crosstalk in the imaging results. Yan and Sava (2008b) suggest applying imaging conditions to separated mode waves, which helps to suppress the artifacts. In general 2D anisotropic media, P- and SV-waves are intrinsically coupled and their polarization directions are no longer parallel or perpendicular to the propagation direction. Many authors have been working on separating P- and S-waves from full elastic waves. The basic idea of wavefield separation method is to project the displacement vector wavefield U onto the polarization vectors of P- and S-waves, which makes the determination of the polarization vectors essential. Rommel (1994) propose to calculate the polarization vectors of qP- and qSV-waves by solving the Christoffel equation with local elastic parameters or Thomsen parameters. (Tsvankin, 2012) propose to calculate the polarization vectors of qP-wave by the rotation of wave vector with a deviation angle, where Thomsen parameters can also apply. Yan and Sava (2008a, 2009) propose a nonstationary separation method for 2D VTI media, which transforms the wavenumber domain operators into space domain and obtain the space domain pseudo-derivative operators, this algorithm will overcome the shortcoming of wavenumber domain method (Dellinger and Etgen, 1990; Dellinger, 1991) and can separate qP- and qS-waves completely even in media with velocity varing spatially. Previous authors have also proposed to directly simulate separated P- and SV-waves in elatic media. Zhang et al. (2007) propose to simulate P- and S-waves with fully decoupled first-order P- and S-wave equations using staggered-grid finite-difference scheme. However, in general anisotropic media, P- and S-waves are intrinsically coupled, which limits the feasibility of this algorithm. In anisotropic media, Cheng and Kang (2013, 2016) derive modified second-order wave equations to simulate separated qP- and qSV-waves for forward modeling, migration and waveform inversion,

which splits wavefield separation procedure into a two-steps scheme. Liu et al. (2018) and Liu and Innanen (2019) propose to further derive the first-order wave equations and develop a first-order qSV-wave propagator in general 2D VTI media using staggered-grid scheme.

In this study, we use a similar strategy to develop a first-order qP-wave propagater in VTI media. Following the principles of (Liu et al., 2018; Liu and Innanen, 2019), we introduce and distribute the velocity fields and stress fields on a 2D staggered grid, in this way staggered-grid scheme can be employed in the first-order equations and corresponding finite difference iterative format can be achieved. In addition, we also adopt the first-order Hybrid-PML Zhang et al. (2014) in our algorithm to help suppress the artificial reflections in the wavefield simulation in strongly anisotropic media. In this paper, we first introduce the theory of this algorithm and derive the first-order equations of qP-waves. Then, we apply this new algorithm to simulate qP-waves in an isotropic medium, VTI media with weak/strong anisotropy and a two-layer VTI model, which validate the feasibility of our algorithm.

First-Order Propagator of Pseudo-Pure-qP-Waves in 2D VTI Media

In 2D isotropic media, scalar P-wave can be separated by applying a dot operation that essentially projects the wavefield $\tilde{U}$ onto the polarization vector a^{qP} in the wavenumber domain (Dellinger and Etgen, 1990; Dellinger, 1991):

$$\tilde{U}^P = \; i\, a^{qP} \cdot \tilde{U}, \tag{1}$$

where $a^{qP} = (a_x^{qP}, a_z^{qP})^T$ is the polarization vector of qP-waves. Cheng and Kang (2013) propose to split this projection separation procedure into a two-steps scheme. First, project the original qP-wavefield onto isotropic references through the introduction of a similarity transformation to Christoffel matrix G

$$\tilde{G}_{qP} = \; M_P \tilde{G}\, M_P^{-1}, \tag{2}$$

where

$$\tilde{G} = \begin{bmatrix} C_{11}\, k_x^2 + C_{44}\, k_z^2 & (C_{13} + C_{44})\, k_x\, k_z \\ (C_{13} + C_{44})\, k_x\, k_z & C_{44}\, k_x^2 + C_{33}\, k_z^2 \end{bmatrix}. \tag{3}$$

and

$$M_P = \begin{bmatrix} i\, k_x & 0 \\ 0 & i\, k_z \end{bmatrix}. \tag{4}$$

Through the similarity transform of Christoffel matrix,

$$\tilde{G}_{qP} = \begin{bmatrix} C_{11}\, k_x^2 + C_{44}\, k_z^2 & (C_{13} + C_{44})\, k_z^2 \\ (C_{13} + C_{44})\, k_x^2 & C_{44}\, k_x^2 + C_{33}\, k_z^2 \end{bmatrix}. \tag{5}$$

In this way, we can derive the equivalent Christoffel equation of qP-waves. through inverse Fourier transform, we obtain the second-order pseudo-pure-qP-wave equations ex-

pressed as below:

$$\begin{aligned}\rho\frac{\partial^2 u_x}{\partial t^2} &= C_{11}\frac{\partial^2 u_x}{\partial x^2} + C_{44}\frac{\partial^2 u_x}{\partial z^2} + (C_{13}+C_{44})\frac{\partial^2 u_z}{\partial z^2}\\ \rho\frac{\partial^2 u_z}{\partial t^2} &= C_{33}\frac{\partial^2 u_z}{\partial z^2} + C_{44}\frac{\partial^2 u_z}{\partial x^2} + (C_{13}+C_{44})\frac{\partial^2 u_x}{\partial x^2}\end{aligned} \tag{6}$$

Zhang and McMechan (2010) pointed out that velocity fields can be separated as well as displacement fields. In this study, we further reduce the order of equations and derive the first-order equations by following procedures. First, we introduce velocity fields v_x and v_z as intermediate variables and let

$$\begin{aligned}\frac{\partial u_x}{\partial t} &= v_x\\ \frac{\partial u_z}{\partial t} &= v_z\end{aligned} \tag{7}$$

Then, we further introduce variables (Liu et al., 2018; Liu and Innanen, 2019): σ_{xx}, σ_{zz} and σ_{xz}, let

$$\begin{aligned}\rho\frac{\partial \sigma_{xx}}{\partial t} &= C_{11}\frac{\partial v_x}{\partial x} - C_{44}\frac{\partial v_z}{\partial z} + (C_{13}+C_{44})\frac{\partial v_z}{\partial x}\\ \rho\frac{\partial \sigma_{zz}}{\partial t} &= C_{33}\frac{\partial v_z}{\partial z} - C_{44}\frac{\partial v_x}{\partial x} + (C_{13}+C_{44})\frac{\partial v_x}{\partial z}\\ \rho\frac{\partial \sigma_{xz}}{\partial t} &= C_{44}(\frac{\partial v_z}{\partial x} + \frac{\partial v_x}{\partial z})\end{aligned} \tag{8}$$

Substituting equation 8 into equation 6, we get:

$$\begin{aligned}\rho\frac{\partial v_x}{\partial t} &= \frac{\partial \sigma_{xx}}{\partial x} + \frac{\partial \sigma_{xz}}{\partial z}\\ \rho\frac{\partial v_z}{\partial t} &= \frac{\partial \sigma_{xz}}{\partial x} + \frac{\partial \sigma_{zz}}{\partial z}\end{aligned} \tag{9}$$

In this way, we derive the first-order pseudo-pure-qP-wave equations. In addition, applying the Thomsen notation (Thomsen, 1986):

$$\begin{aligned}C_{11} &= (1+2\epsilon)\rho\, v_{p0}^2\\ C_{33} &= \rho\, v_{p0}^2\\ C_{44} &= \rho\, v_{s0}^2\\ \rho\, v_{pn}^2 &= \rho\, v_{p0}^2\sqrt{(1+2\delta)}\\ (C_{33}+C_{44})^2 &= \rho^2(\, v_{p0}^2 - \, v_{s0}^2)(\, v_{pn}^2 - \, v_{s0}^2)\end{aligned} \tag{10}$$

the first-order Pseudo-pure-qP-wave equations can be rewritten as below:

$$
\begin{aligned}
\rho\frac{\partial\sigma_{xx}}{\partial t} &= (1+2\epsilon)\rho\, v_{p0}^2\frac{\partial\, v_x}{\partial x} - \rho\, v_{s0}^2\frac{\partial\, v_z}{\partial z} + \sqrt{\rho^2(\, v_{p0}^2 - \, v_{s0}^2)(\, v_{pn}^2 - \, v_{s0}^2)}\frac{\partial\, v_z}{\partial x}\\
\rho\frac{\partial\sigma_{zz}}{\partial t} &= \rho\, v_{p0}^2\frac{\partial\, v_z}{\partial z} - \rho\, v_{s0}^2\frac{\partial\, v_x}{\partial x} + \sqrt{\rho^2(\, v_{p0}^2 - \, v_{s0}^2)(\, v_{pn}^2 - \, v_{s0}^2)}\frac{\partial\, v_x}{\partial z}\\
\rho\frac{\partial\sigma_{xz}}{\partial t} &= \rho\, v_{s0}^2(\frac{\partial\, v_z}{\partial x} + \frac{\partial\, v_x}{\partial z})\\
\rho\frac{\partial\, v_x}{\partial t} &= \frac{\partial\, \sigma_{xx}}{\partial x} + \frac{\partial\, \sigma_{xz}}{\partial z}\\
\rho\frac{\partial\, v_z}{\partial t} &= \frac{\partial\, \sigma_{zx}}{\partial x} + \frac{\partial\, \sigma_{zz}}{\partial z}
\end{aligned}
\tag{11}
$$

What's also worthy to note is that v_x and v_z grid points are half a grid away from each other in both x- and z-axis directions in a 2D staggered grid. Therefore, v_x or v_z field should be phase shifted before the filtering algorithm is performed (Liu and Innanen, 2019). There will still be some residual qSV-wave energy in the wavefields simulated by these first-order qP-wave equations. Applying the same filtering algorithm (Cheng and Kang, 2013), we can obtain pure scalar qP-waves.

Simulation Examples of Separated Scalar qP-Waves

In this paper, we present the synthetic examples using the same models in Liu and Innanen (2019). Also, we simulate qP-wave propagation by both original elastic wave equations and first-order pseudo-pure-qP-wave equations proposed in this study for comparison.

Homogeneous isotropic medium

We first simulate the wavefields propagating in a homogeneous isotropic medium with size of $2\ km \times 2\ km$, whose density is 2500 kg/m^3, P-wave velocity is 4000 m/s and S-wave velocity is 2300 m/s. The Ricker wavelet source is loaded at v_x grid point right in the middle of the model. The normalized x- and z-components of wavenumber K for a homogeneous isotropic medium are shown in Fig 1, which are also the polarization direction components of P-wave in isotropic media.

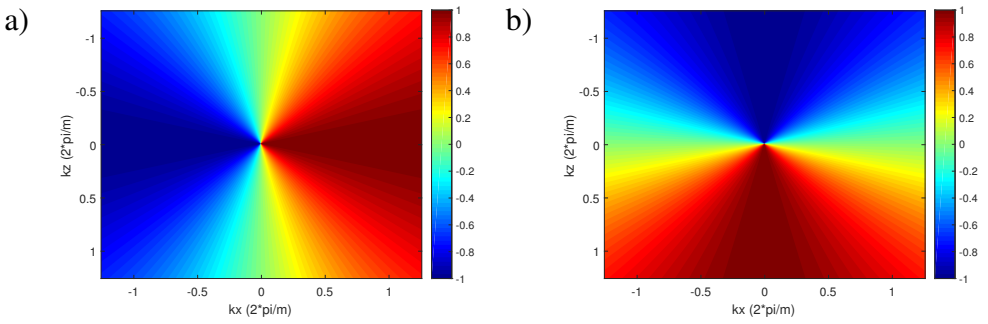

FIG. 1. Normalized wavenumber-domain operators in 2D isotropic medium: a) kx and b) kz.

The synthetic wavefields are shown in Fig 2. a) and b) are x- and z-components simulated by original elastic wave equations. c) and d) are x- and z-components simulated by first-order pseudo-pure-qP-wave equations. What's obvious is that the x- and z-components of SV-wave are in totally opposite phase, by summing up these two components, we can eliminate the SV-wave energy and obtain a scalar P-wave (shown in Fig 2 e)); f) is scalar P-wave filtered with deviation operators, which is the identical with e). because P-wave propagates parallelly to the polarization direction and $a^P = K$ in an isotropic medium.

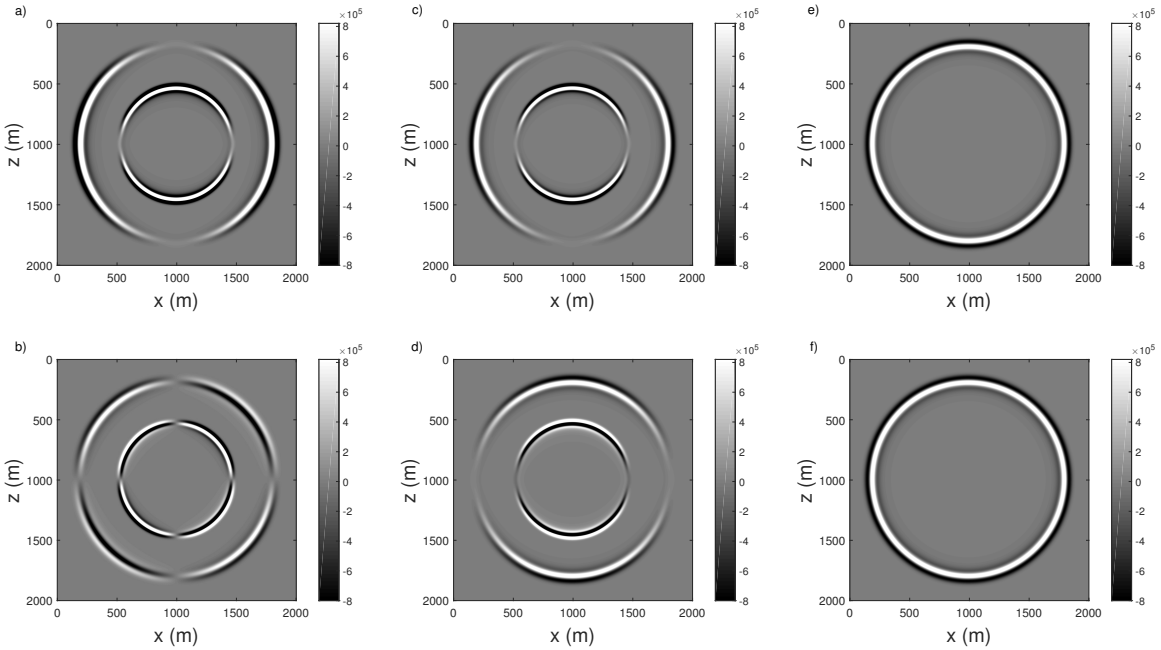

FIG. 2. Synthetic wavefields in an isotropic medium: a) x- and b) z-component simulated by original elastic wave equations; c) x- and d) z-components simulated by first-order pseudo-pure-qP-wave equations; e) summation of qP-wave components; f) separated scalar qP-wave.

Homogeneous VTI medium with weak anisotropy

In the second case, we apply the algorithm to a homogeneous VTI medium with weak anisotropy. The Thomsen parameters are as follows: $vp_0 = 3000\ m/s$, $vs_0 = 1500\ m/s$, $\epsilon = 0.1$ and $\delta = 0.05$. Using Rommel's (Rommel, 1994) method, we calculate the normalized x- and z-components of wavenumber domain and corresponding spatial domain deviation operators, which are shown in Fig 3 and Fig 4, respectively.

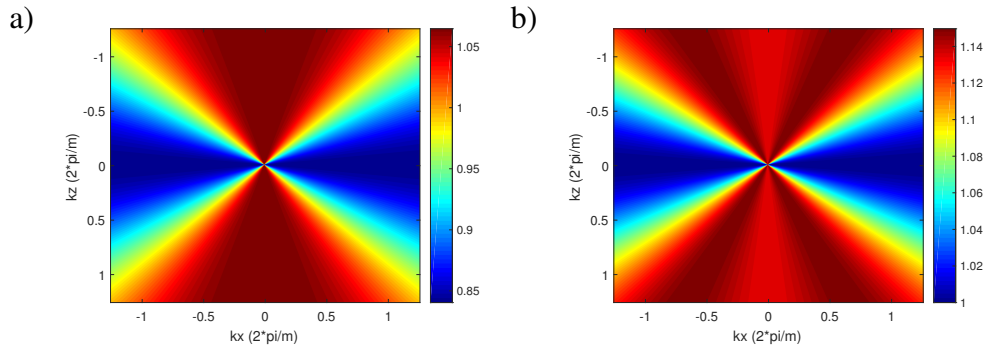

FIG. 3. Normalized wavenumber-domain operator in 2D VTI medium with weak anisotropy: a) x- and b) z-component of deviation operator.

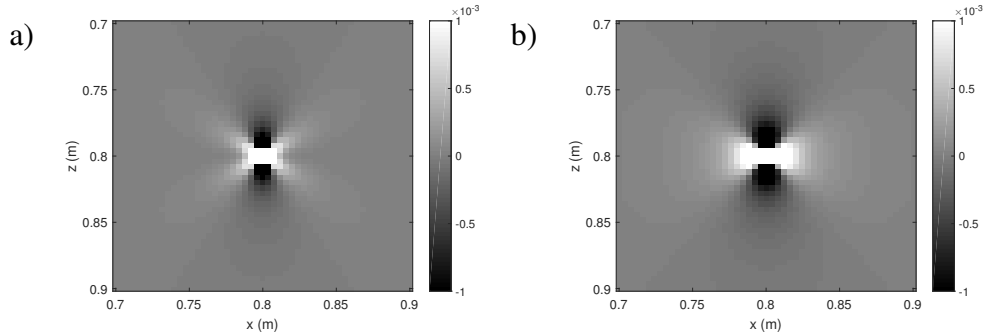

FIG. 4. Spatial domain deviation operator in 2D VTI medium with weak anisotropy: a) x-component; b) z-component.

The synthetic wavefields in VTI medium are shown in Fig **??**: a) and b), c) and d) are respectively the x- and z-components of the velocity wavefields simulated by original elastic wave equations and first-order qP-wave equations. The x- and z-components of qSV-wavefields in c) and d) are in different phases, the summation e) enhances qP-waves in VTI media, while leaving some resigual qSV-wave energy in the physical domain. Since this is also a homogeneous model, we can perform the filtering algorithm with either the wavenumber domain or the spatial domain deviation operators to the synthetic wavefields, as shown in f) is the separated scalar qP-wave, where qSV-wave energy is completely removed with the projection deviation correction.

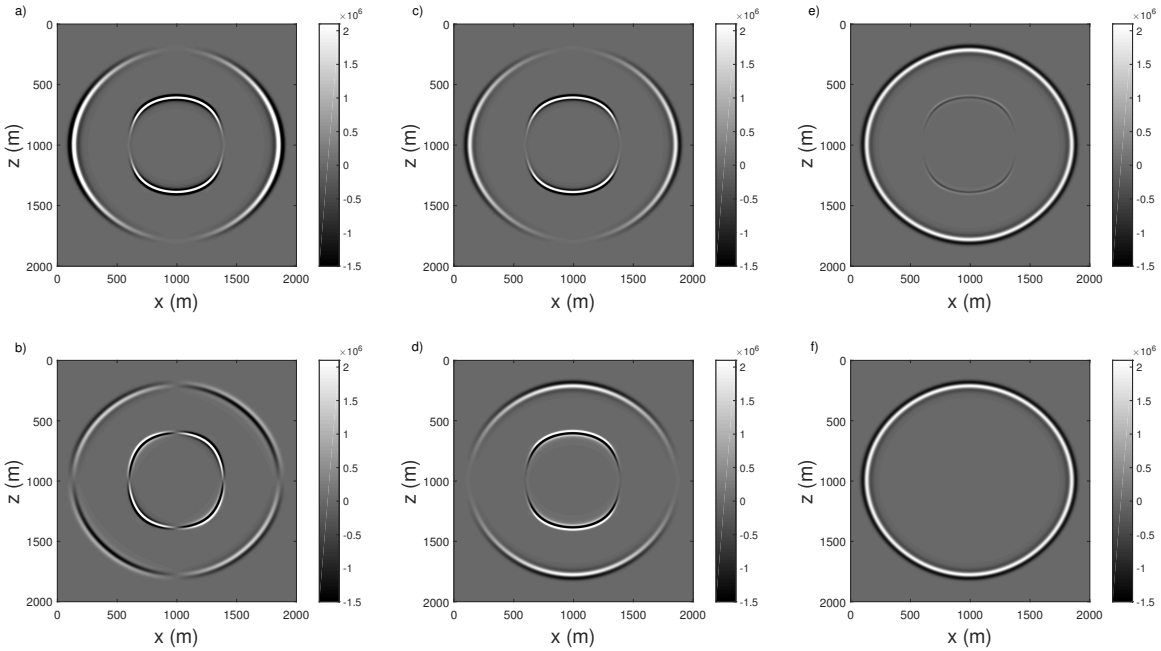

FIG. 5. Synthetic wavefields in a VTI medium with weak anisotropy: a) x- and b) z-component simulated by original elastic wave equations; c) x- and d) z-component simulated by first-order pseudo-pure-qP-wave equations; e) summation of qP-wave components; f) separated scalar qP-wave.

Homogeneous VTI medium with strong anisotropy

In the third case, we apply the new algorithm to a VTI medium with strong anisotropy, whose elastic parameters: C_{11} is 23.87 GPa, C_{33} is 15.33 GPa, C_{13} is 9.79 GPa, C_{44} is 2.77 GPa and density is $2500kg/m^3$. The synthetic wavefields are shown in Fig 6. From the comparison between Fig 6 e) and f), we can see the qSV-wave energy can also be completely eliminated and scalar pseudo-qP-wave can be obtained after the filtering algorithm.

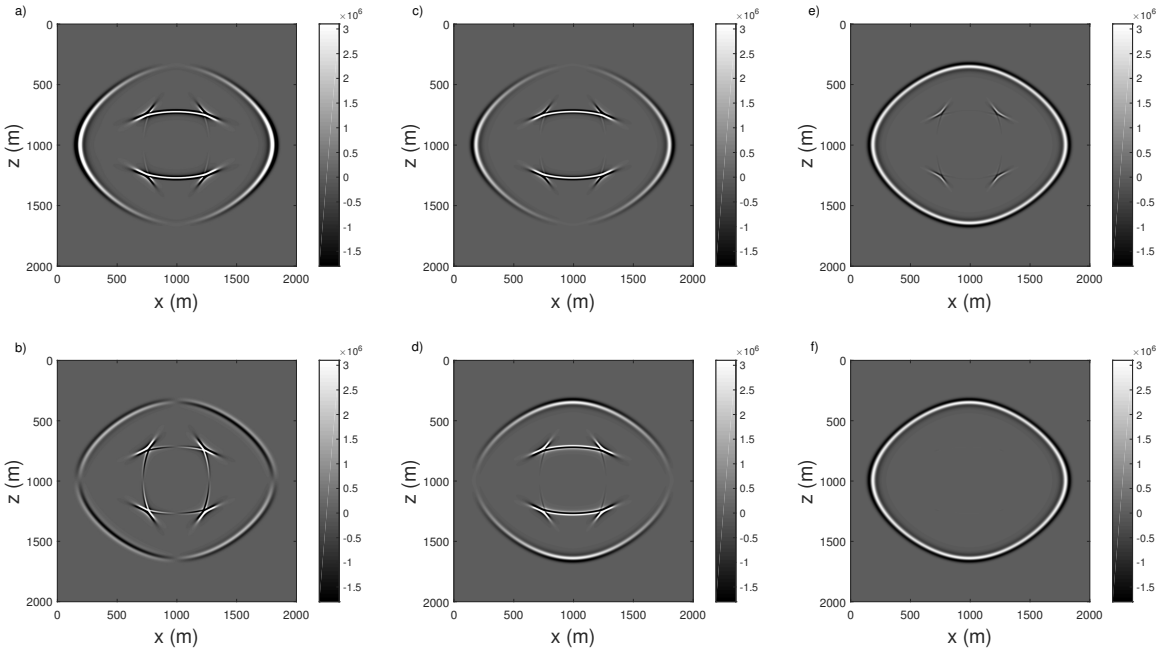

FIG. 6. Synthetic wavefields in a VTI medium with strong anisotropy: a) x- and b) z-component simulated by original elastic wave equations; c) x- and d) z-component simulated by first-order pseudo-pure-qP-wave equations; e) summation of qP-wave components; f) separated scalar qP-wave.

Here we present the snapshots of synthetic qP-wavefields simulated by first-order Pseudo-pure-qP-wave equations to validate the applicability of the first-order Hybrid-PML (Zhang et al., 2014). As shown in Fig 7 a), b) and c) are the snapshots of x-component of qP-wavefields propagating at 320 ms, 400 ms and 480 ms, respectively. We can notice that the Hybrid-PML implemented in our algorithm provides satisfactory performance.

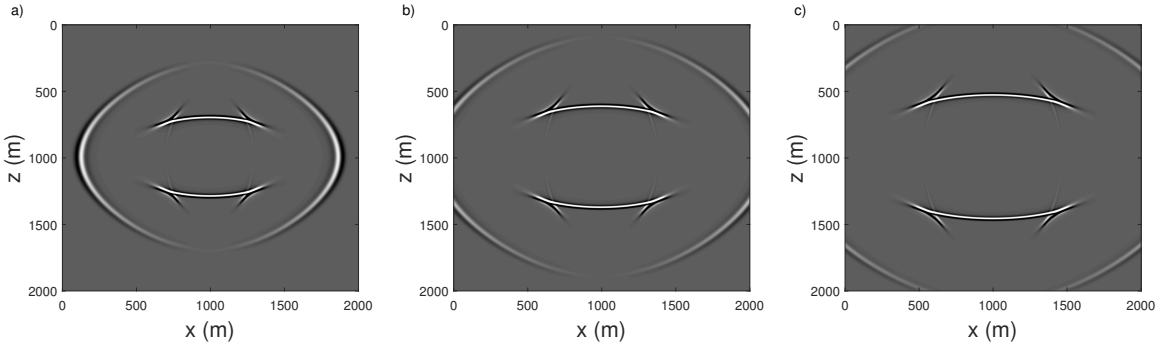

FIG. 7. Snapshots of x-component simulated by first-order qP-wave equations in a VTI medium with strong anisotropy: a) 320 ms, b) 400 ms and c) 480 ms, respectively.

Heterogeneous layered VTI media

In the last case, we simulate the qP-wavefields in a heterogeneous two-layer VTI model, in which the first and the second layer are the same VTI medium with strong and weak anisotropy, respectively. The force source is also located right in the middle of the model

with the interface at depth of 1.2 km. Synthetic qP-wavefields are shown in Fig 8. We can notice the converted S-wavefields emerge at the interface. By the summation of x- and z-components of synthetic qSV-wavefields shown in Fig 8 e), some of S-wavefields are already seriously suppressed. In this heterogeneous model, we have to perform the filtering algorithm using the spacial domain deviation operators, after which all residual qSV-wave energy is eliminated and pure scalar qP-wave is obtained as shown in Fig 8 f).

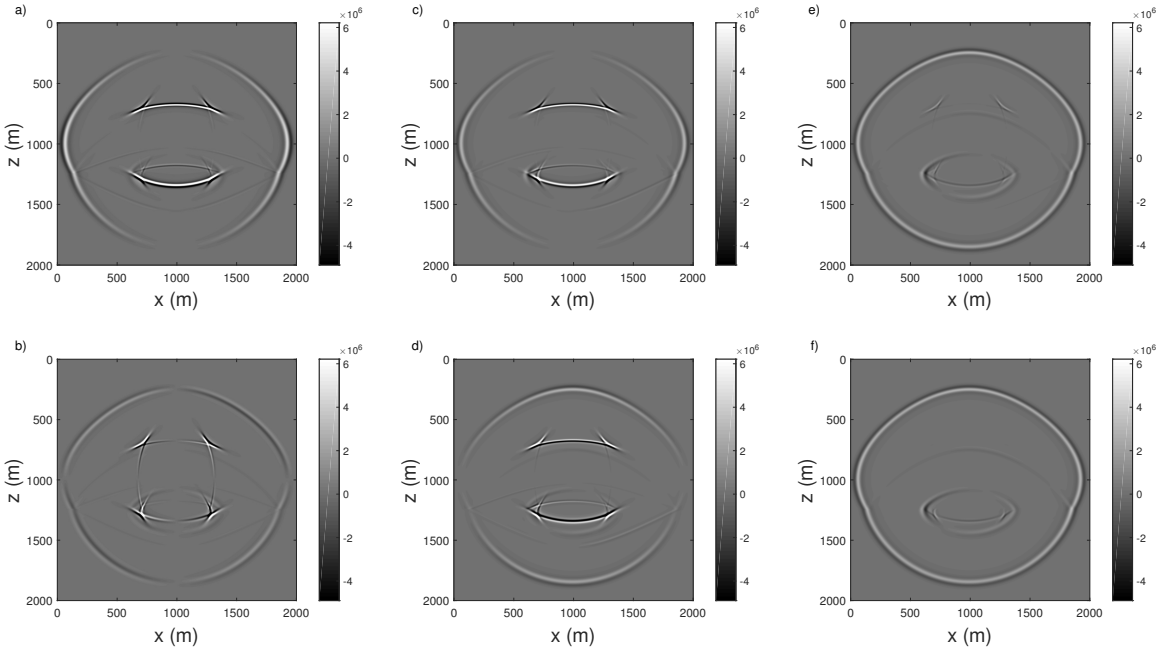

FIG. 8. Synthetic wavefields in a layered VTI model: a) x- and b) z-component simulated by original elastic wave equations; c) x- and d) z-component simulated by first-order pseudo-pure-qP-wave equations; e) summation of qP-wave components; f) separated scalar qP-wave.

CONCLUSIONS

In this study, through introducing intermediate variables, we propose an alternative algorithm based on staggered-grid scheme to simulate qP-wave in general 2D VTI media. Since the first-order qP-wave equations keep very similar form of those of the first-order elastic wave equations, we can achieve the new algorithm with very simple modification to existing first-order elastic wave simulation program. Similar to our first-order qSV-wave propagator, we also need to phase shift the velocity fields before performing the filtering algorithm. We have applied the proposed algorithm to a homogeneous isotropic medium, homogeneous anisotropic VTI media with weak/strong anisotropy and a heterogeneous layered VTI model, the synthetic wavefields of which need to be further corrected to remove residual qSV-wave energy. Through the synthetic examples, it's demonstrated that the algorithm is capable of simulating qP-wave propagation in general VTI media.

ACKNOWLEDGMENTS

We thank the sponsors of CREWES for continued support. This work was funded by CREWES industrial sponsors, NSERC (Natural Science and Engineering Research Council of Canada) through the grants CRDPJ 461179-13 and CRDPJ 543578-19. Partial funding

also came from the Canada First Research Excellence Fund.

REFERENCES

Chang, W., and McMechan, G., 1987, Elastic reverse-time migration: Geophysics.

Cheng, J., and Kang, W., 2013, Simulating propagation of separated wave modes in general anisotropic media, part i: qp-wave propagators: Geophysics, **79**, No. 1, C1–C18.

Cheng, J., and Kang, W., 2016, Simulating propagation of separated wave modes in general anisotropic media, part ii: qs-wave propagators: Geophysics, **81**, No. 2, C39–C52.

Dellinger, J., and Etgen, J., 1990, Wave-field separation in two-dimensional anisotropic media: Geophysics, **55**, No. 7, 914–919.

Dellinger, J. A., 1991, Anisotropic seismic wave propagation, vol. 69: Stanford University Stanford.

Liu, H., and Innanen, K., 2019, A first-order quasi-sv-wave propagator in 2-dimensional vertical transversely isotropic (vti) media: Crewes research report,, **31**, 39.1–39.4.

Liu, H., Wang, B., Ali, M., Tao, G., Yue, W., and Sun, H., 2018, A first-order qsv-wave propagator in 2d vti media, *in* 80th EAGE Conference and Exhibition 2018.

Rommel, B. E., 1994, Approximate polarization of plane waves in a medium having weak transverse isotropy: Geophysics, **59**, No. 10, 1605–1612.

Thomsen, L., 1986, Weak elastic anisotropy: Geophysics, **51**, No. 10, 1954–1966.

Tsvankin, I., 2012, Seismic signatures and analysis of reflection data in anisotropic media: Society of Exploration Geophysicists.

Yan, J., and Sava, P., 2008a, Elastic wavefield separation for vti media, *in* SEG Technical Program Expanded Abstracts 2008, Society of Exploration Geophysicists, 2191–2195.

Yan, J., and Sava, P., 2008b, Isotropic angle-domain elastic reverse-time migration: Geophysics, **73**, No. 6, S229–S239.

Yan, J., and Sava, P., 2009, Elastic wave-mode separation for vti media: Geophysics, **74**, No. 5, WB19–WB32.

Zhang, J., Zhenping, T., and Chengxiang, W., 2007, P-and s-wave-separated elastic wave-equation numerical modeling using 2d staggered grid, *in* SEG Technical Program Expanded Abstracts 2007, Society of Exploration Geophysicists, 2104–2109.

Zhang, K., Tao, G., Li, J., Wang, H., Liu, H., and Ye, Q., 2014, 3d fdm modeling of acoustic reflection logging in a deviated well, *in* 76th EAGE Conference and Exhibition 2014.

Zhang, Q., and McMechan, G. A., 2010, 2d and 3d elastic wavefield vector decomposition in the wavenumber domain for vti media: Geophysics, **75**, No. 3, D13–D26.